SUPPLEMENTARY INFORMATION

Characterization of Spatial Distribution of Dipeptides Enabled by MALDI MSI with On-tissue Derivatization

Kening Li‡[a], Shuai Guo‡[b], Weiwei Tang*[a], Bin Li*[a]

[1] State Key Laboratory of Natural Medicines and School of Traditional Chinese Pharmacy, China Pharmaceutical University, Nanjing, 210009, China

[2] School of Basic Medicine and Clinical Pharmacy, China Pharmaceutical University, Nanjing, 210009, China

EXPERIMENTAL SECTION

Chemicals. Hexafluoroisopropanol (1,1,1,3,3,3-hexafluoro-2-propanol, HFIP), α-cyano-4-hydroxycinnamic acid (CHCA), and glycyl-glycine were obtained from Shanghai Yuanye Biotechnology (Shanghai, China). 1,1,1-Trifluoro-2-propanol (TFIP) and isopropanol (ISP) were purchased from Macklin (Shanghai, China). 4-Hydroxy-3-methoxycinnamaldehyde (CA) and trifluoroacetic acid (TFA) were purchased from Sigma-Aldrich (St. Louis, MO). LC-MS grade methanol (MeOH) and acetonitrile (ACN) were purchased from Merck (Darmstadt, Germany). Deionized water was obtained from a Milli-Q system (Millipore, Burlington, MA).

Tissue Preparation and Sectioning. Male 1 to 3-month-old Sprague-Dawley rats, and male 8-week-old wild-type and *ob/ob* C57 mice were purchased from Xipuer-BiKai (Shanghai, China). Animals were maintained in an environmentally controlled breeding room (12 h dark/light cycle at 24 °C) for at least one week before experiments. Animal experiments were conducted following the Guidelines for Animal Experimentation of China Pharmaceutical University (Nanjing, China), and approved by the Animal Ethics Committee of this institution. Tissues were harvested from the sacrificed animals, followed by the quick-frozen on dry ice, and stored at -80 °C until use. The 12 μm thick tissue sections were obtained at -20 °C using a cryostat (Leica CM3050, Germany) and thaw-mounted onto the conductive indium-tin-oxide (ITO) coated glass slide.

On-tissue Chemical Derivatization Using the LACT System. The LACT system, described in detail elsewhere,[1] was based on a diode laser source (405 nm, LSR405SD, Lasever, China) and a 2D translation stage (EB100, Haijie Technology Co., Beijing, China) controlled by an in-house written software. The solution of CA (20 mg/mL in 50% MeOH), CHCA (30 mg/mL in 80% ACN), fluorine-containing reagent and TFA were mixed in ratio 1:1:0.1:0.004 (v/v/v/v) and sprayed on the tissue section using an electric-assisted sprayer assembled in LACT system. A high voltage (6.0 kV) was added between the spray emitter and ITO glass slide to generate a stable Taylor cone with the aid of the N_2 gas (11.5 psi). After homogenous deposition of the prepared mixture, the tissue slide (donor slide) was placed on the top of a clean ITO slide (acceptor slide) in a face-to-face manner (gapless) and mounted on a 2D translation stage. The LACT process was performed by continuously illuminating the backside of the tissue slide in the *x*-direction using a focused diode laser. Correspondingly, each step in the *y*-direction was between 150 μm. Under the optimized laser power (~5 mW), the laser beam was focused on the matrix layer (CHCA), and a strongly localized heat was generated, causing volatilization and ejection of a small volume of matrix-analyte mixture to be ablated from the donor slide onto the acceptor slide to form a thin chemical film. The two slides were easily separated, and no external force is needed to break two slides apart after the LACT experiment. Subsequently, the acceptor slide (chemical film) was subjected to MALDI MSI. The chemical film generated was directly analyzed by MALDI MSI without additional sample preparation.

MALDI MSI. All MALDI MSI experiments were carried out on an ultrafleXtreme MALDI TOF-TOF MS (Bruker Daltonics) equipped with a Nd:YAG solid-state Smartbeam II laser (λ=355 nm). The laser was set to the "Ultra" footprint setting at a ~100 μm diameter. Mass calibration was achieved using CHCA matrix peaks, CA-derivatized Gly-Gly, and a Peptide Calibration Standard Kit II (Bruker Daltonics, USA). All tissues were analyzed with 100 laser shots fired at 1000 Hz and imaged with a 200 μm laser step size. The mass spectra were acquired in the positive ion mode with an *m/z* range of 50-600. *In situ* MALDI LIFT TOF-TOF MS/MS analysis was performed to confirm the structure of the derivatized dipeptides. In addition, accurate *m/z* was acquired for dipeptide identification using a high mass resolution 7T SolariX Fourier transform ion cyclotron resonance (FTICR) mass spectrometer equipped with a dual MALDI and ESI source (Bruker Daltonics).

LC-MS/MS Validation. To confirm MALDI MSI results, punch-sampled tissues collected from specific regions of the brain and liver were analyzed using LC-MS/MS. Brain tissue was punched with a tissue punch (1 mm i.d.) at selected regions, including cerebral cortex (CTX), hippocampal (HIP), thalamus (THA), hypothalamus (HTH), striatum (STR), and cerebellum (CER). Similarly, the specific regions of liver tissues were punch sampled from the wide-type and *ob/ob* C57 mice, respectively. The punched tissues were homogenized in cold normal saline (1:5, w/v). After sonication for 15 min, 60 μL of each homogenate was mixed with 300 μL methanol containing 10 ng/mL ornithly-tyrosine (Orn-Tyr) (IS), vortexed for 5 min, and centrifuged at 13000 ×g for 10 min at 4 °C. 4 μL of each respective supernatant was injected into the LC-MS/MS system.

LC-MS/MS was performed using an Agilent 6520 Q-TOF mass spectrometer connected to an Agilent 1260 series UHPLC system (Agilent Technologies, CA). Target dipeptides were separated on an Agilent XDB C18 column (3.0 mm × 50 mm,1.8 μm) preceded by a guard column (Agilent Eclipse XDB-C18, 5 mm × 4.6 mm, 1.8 μm). The mobile phase A was H_2O containing 0.1% formic acid and phase B was ACN. The flow rate was 0.4 mL/min, and the gradient program was conducted as follows: 0-3 min, 1-10% B; 3-6 min, 10-50% B; 6-9 min, 50-95% B; 9-12 min, 95% B; 12-14 min, 95-1% B. The injection volume was 4 μL, and the column temperature was kept at 35 °C. The mass spectrometer was operated in the positive ion mode and the ESI source parameters were as follows: dry gas temperature, 350 °C; dry gas flow, 10 L/min; nebulizer pressure, 30 psi; sheath gas temperature, 300 °C; sheath gas flow, 12 L/min; capillary voltage, 3.5 kV.

Data Analysis. MALDI MSI data was read and analyzed using flexAnalysis 3.4 and flexImaging 4.1 (Bruker Daltonics). The peak intensities from different tissue regions of interest (ROI) were extracted using MSiReader v1.00 via the WM Keck FTMS Laboratory. Multivariable statistical analyses were performed using MetaboAnalyst 5.0 online software (www.metaboanalyst.ca) and OriginPro 2017 (OriginLab Corporation, Northampton, MA).

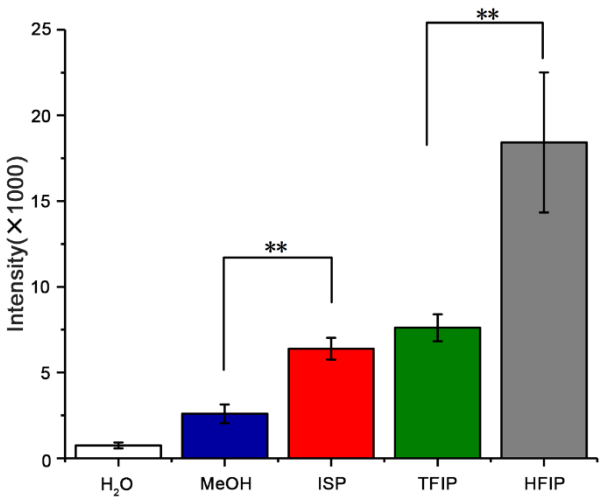

Figure S1. Signal intensities of CA-derivatized Gly-Gly obtained under different solvent compositions. Error bars indicate the standard deviations of 10 mass spectra acquired from the respective ion. Significance levels: ** $p<0.01$.

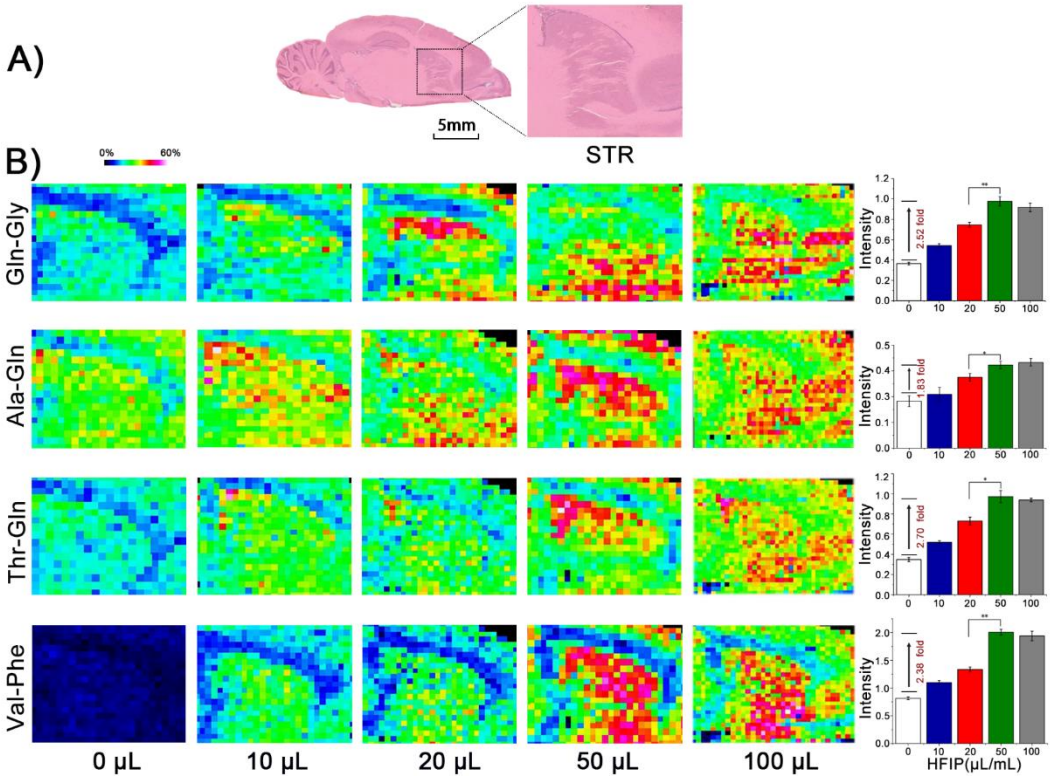

Figure S2. Influence of the amount of HFIP added in the CHCA/CA/TFA mixture on signal intensity of CA derivatized dipeptide. (A) H&E-stained image of the rat brain tissue. (B) Ion images and the average intensity of 4 CA-dipeptides obtained at different amounts of HFIP. Error bars indicate the standard deviations of 20 mass spectra acquired from the respective ion. Significance levels: $^{**}p<0.01$, $^{*}p<0.05$.

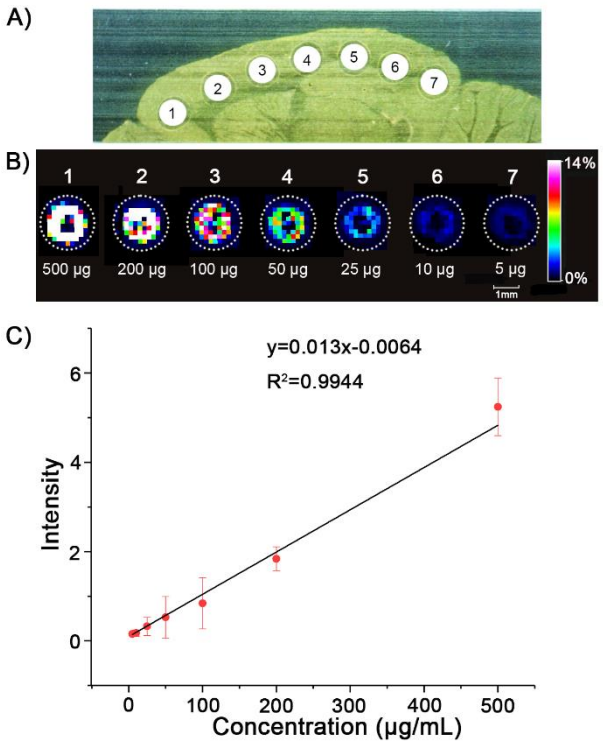

Figure S3. Quantitative calibration curve of CA-Gly-Gly obtained from HFIP-LACT treated brain tissue sections using MALDI MSI. Error bars indicate the standard deviations of 50 mass spectra acquired from the respective ion.

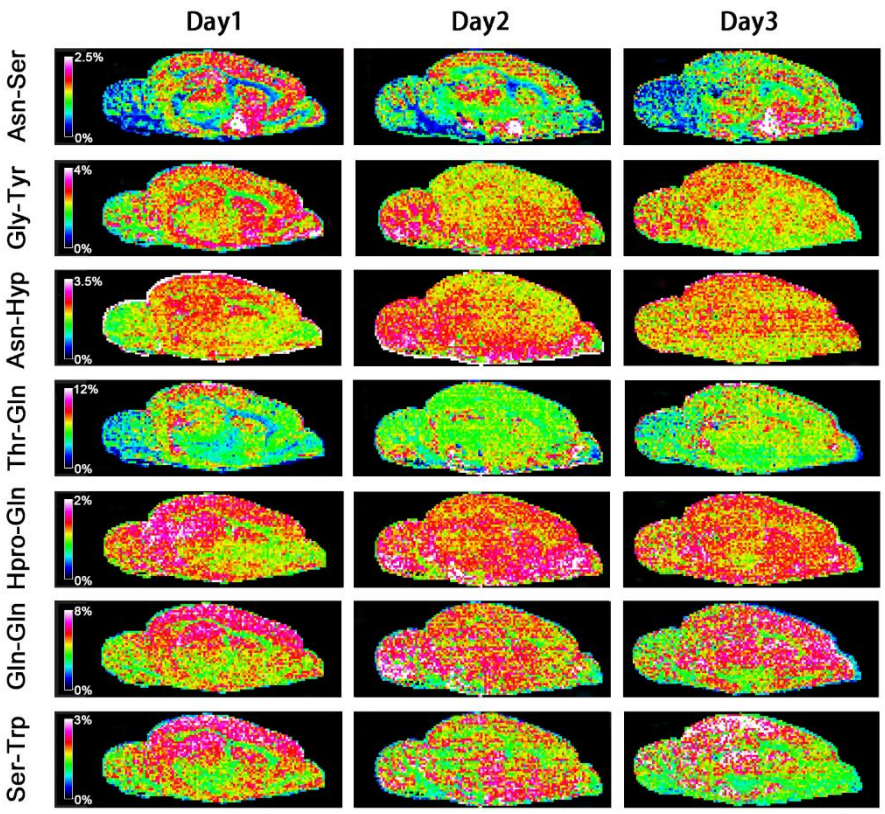

Figure S4. Day-to-day repeatability of MALDI MSI with HFIP-LACT experiments.

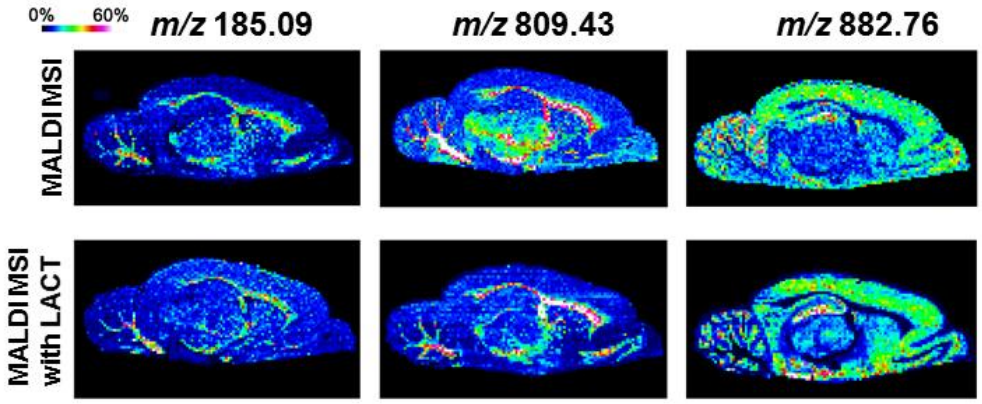

Figure S5. Comparison of spatial distribution patterns of selected ions obtained from rat brain tissue treated without and with LACT by using MALDI MSI.

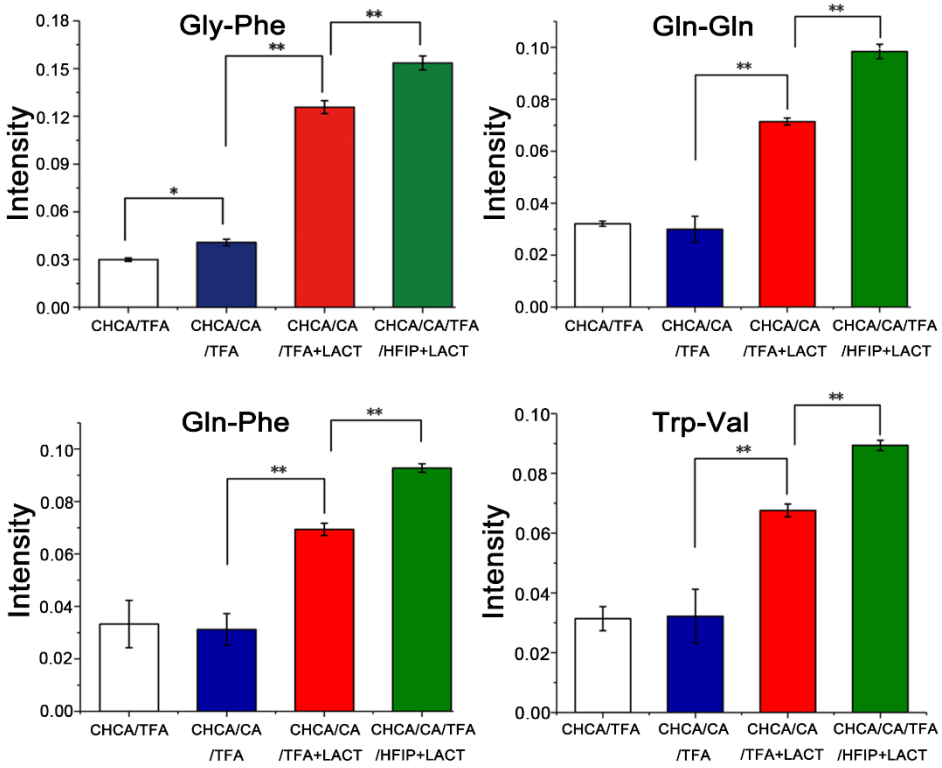

Figure S6. The average intensity of 4 CA-dipeptides, with the standard deviations shown as error bars, obtained from different approaches (n=3). Significance levels: $^{**}p<0.01$, $^{*}p<0.05$.

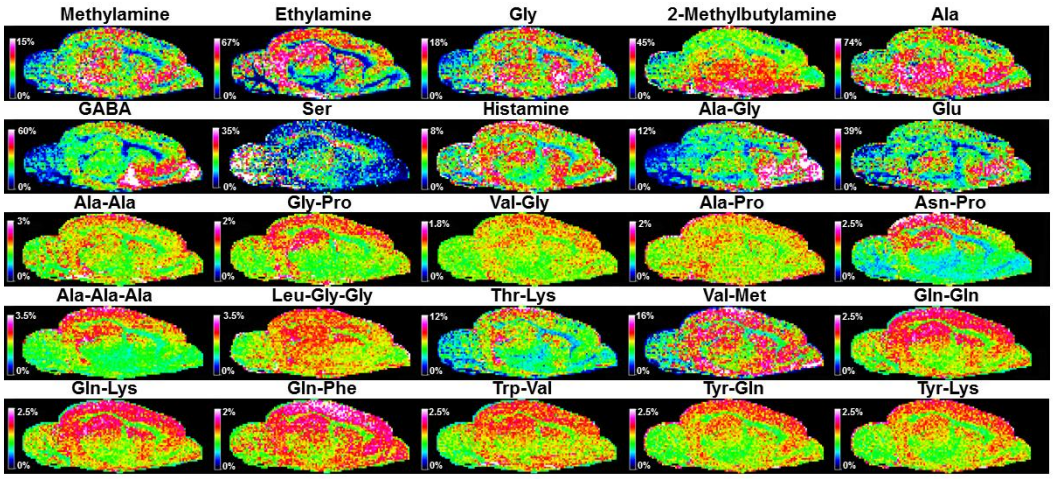

Figure S7. Ion images of selected dipeptides and other primary amine metabolites obtained from the sagittal section of the rat brain using MALDI MSI with HFIP-LACT. Data were acquired at a spatial resolution of 200 μm.

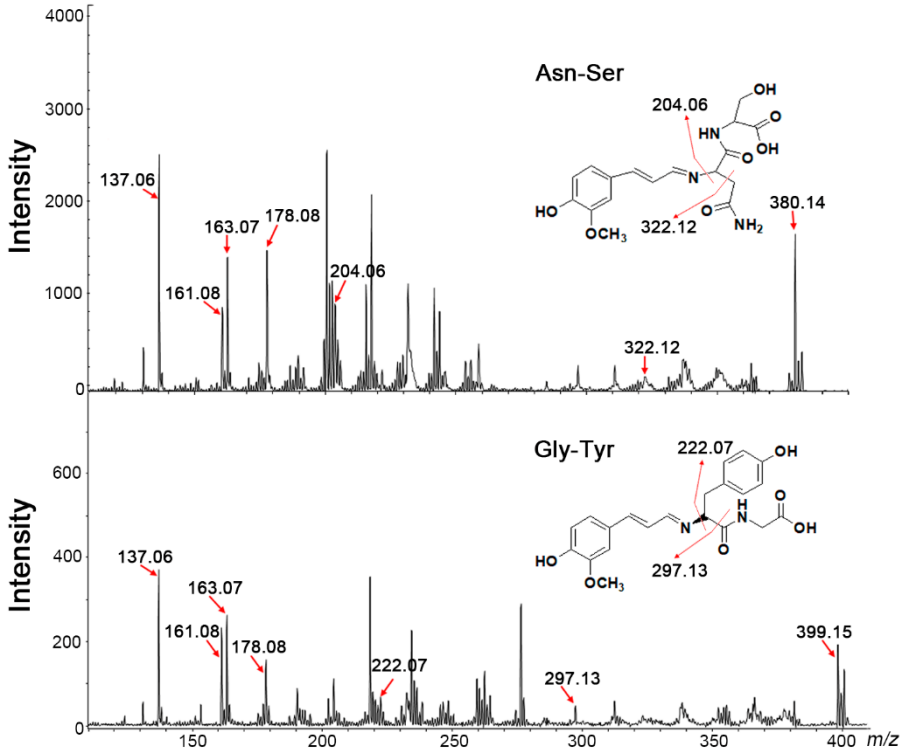

Figure S8. Representative MALDI LIFT ToF-ToF MS/MS spectra of CA-Asn-Ser (*m/z* 380.14) and CA-Gly-Tyr (*m/z* 399.15).

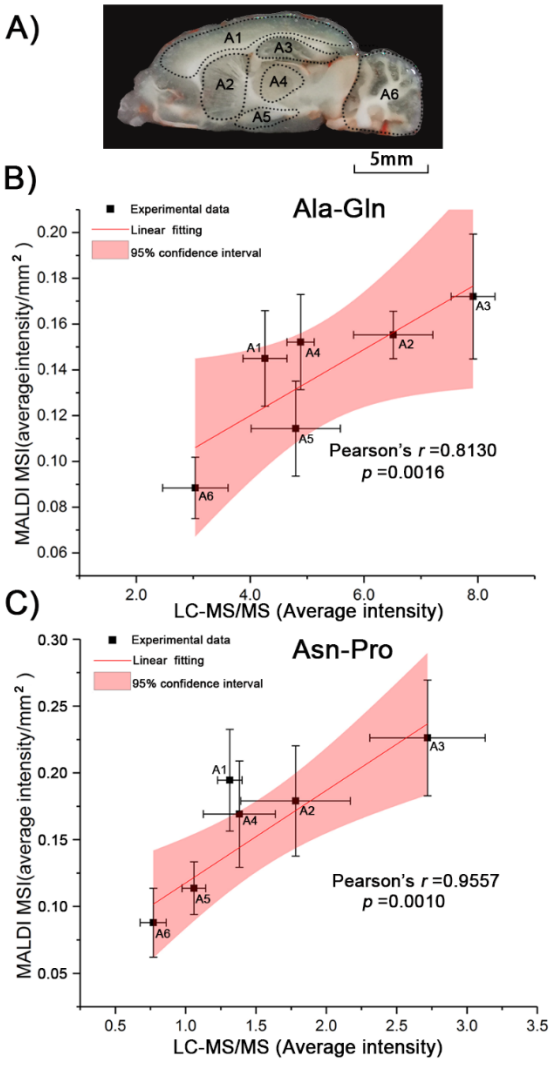

Figure S9. LC-MS/MS validation of the tissue-specific distribution of dipeptides in brain tissues. (A) Tissue punches collected from different regions were used for the LC−MS/MS analyses and MSI ion images of dipeptides. A1 (cerebral cortex, CTX), A2 (striatum, STR), A3 (hippocampus, HIP), A4 (thalamus, THA), A5 (hypothalamus, HTH), A6 (cerebellum, CER). (B) and (C) Correlation of the intensities of two dipeptides in different regions determined by MALDI MSI and LC-MS/MS. Error bars indicate the standard deviations of biological triplicates (n=3).

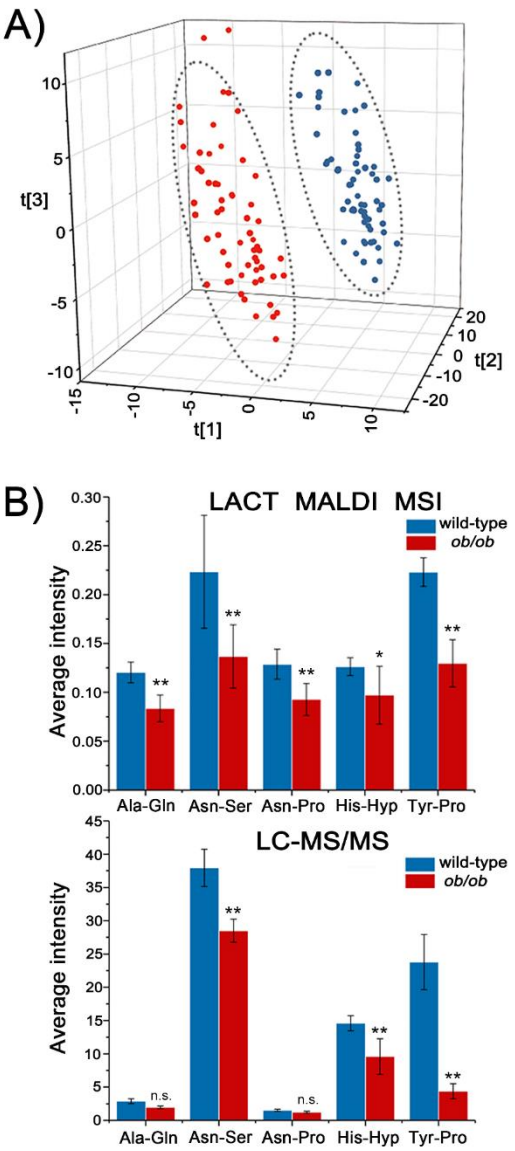

Figure S10. (A) PLS-DA score plot derived from signal intensities of the dipeptide. Red dots: liver of wild-type mice (n=3), blue dots: liver of ob/ob mice (n=3) . (B) Relative intensity of Ala-Gln, Asn-Ser, Asn-Pro, His-Hyp, and Tyr-Pro from wild-type and the ob/ob mouse liver with MALDI MSI (upper) and LC-MS/MS (lower). Error bars indicate the standard deviation of three biological triplicates. Significance levels: ** $p<0.01$, * $p<0.05$, n.s.: no significance. NB: dipeptide isomer may occur.

Table S1. CA-derivatized dipeptides, primary amine metabolites, and tripeptides detected in rat brain tissue using MALDI FTICR MS with HFIP-LACT.

	No.	Matched Metabolites	Molecular Formula	Observed *m/z*	Theoretical *m/z*	Ion Form	Error ppm	MS/MS fragments
Dipeptides	1	Ala-Gly	$C_{15}H_{18}N_2O_5$	307.1289	307.1288	$[M+H]^+$	0.2	137,161,163,178,232,262
	2	Ala-Ala	$C_{16}H_{20}N_2O_5$	321.1447	321.1444	$[M+H]^+$	0.9	137,161,163,178,303
	3	Gly-Pro	$C_{17}H_{20}N_2O_5$	333.1445	333.1444	$[M+H]^+$	0.3	
	4	Val-Gly	$C_{17}H_{22}N_2O_5$	335.1597	335.1601	$[M+H]^+$	-1.2	137,161,163,178,290,261,318
	5	Ala-Pro	$C_{18}H_{22}N_2O_5$	347.1604	347.1601	$[M+H]^+$	0.9	137,161,163,178,234
	6	Gln-Gly	$C_{17}H_{21}N_3O_6$	364.1503	364.1503	$[M+H]^+$	0.0	137,161,163,178,204,318
	7	Ala-Gln	$C_{18}H_{23}N_3O_6$	378.1659	378.1660	$[M+H]^+$	-0.3	137,161,163,178,204,232,242
	8	Asn-Ser	$C_{17}H_{21}N_3O_7$	380.1452	380.1452	$[M+H]^+$	0.0	137,161,163,178,204,322
	9	Gly-Phe	$C_{21}H_{22}N_2O_5$	383.1604	383.1601	$[M+H]^+$	0.8	137,161,163,178,204,222,367
	10	Ala-His	$C_{19}H_{22}N_4O_6$	387.1666	387.1664	$[M+H]^+$	0.8	
	11	Asn-Pro	$C_{19}H_{23}N_3O_6$	390.1660	390.1660	$[M+H]^+$	0.0	137,161,163,178,346,
	12	Val-Asn	$C_{19}H_{25}N_3O_6$	392.1816	392.1816	$[M+H]^+$	0.0	137,161,163,178,204,216,218,348
	13	Thr-Asn	$C_{18}H_{23}N_3O_7$	394.1610	394.1609	$[M+H]^+$	0.3	137,161,163,178,218,234,277
	14	Gly-Tyr	$C_{21}H_{22}N_2O_6$	399.1548	399.1551	$[M+H]^+$	-0.8	137,161,163,178,222,297
	15	Asn-Hyp	$C_{19}H_{23}N_3O_7$	406.1612	406.1609	$[M+H]^+$	0.7	137,161,163,178,217,232,247
	16	Thr-Gln	$C_{19}H_{25}N_3O_7$	408.1766	408.1765	$[M+H]^+$	0.2	137,161,163,178,218,232,247,336,363
	17	Thr-Lys	$C_{20}H_{29}N_3O_6$	408.2127	408.2129	$[M+H]^+$	-0.5	

	18	Val-Met	$C_{20}H_{28}N_2O_5S$	409.1798	409.1791	$[M+H]^+$	1.7	137,161,163,178,218,232,247,366
	19	Met-Thr	$C_{19}H_{26}N_2O_6S$	411.1589	411.1584	$[M+H]^+$	1.2	137,161,163,178,218,367
	20	His-Thr	$C_{20}H_24N_4O_6$	417.1765	417.1769	$[M+H]^+$	-1.0	
	21	Hpro-Gln	$C_{20}H_{25}N_3O_7$	420.1275	420.1265	$[M+H]^+$	2.4	
	22	Asn-Lys	$C_{20}H_{28}N_4O_6$	421.2082	421.2082	$[M+H]^+$	0.0	137,161,163,178,190,246,350
	23	Val-Phe	$C_{24}H_{28}N_2O_5$	425.2074	425.2071	$[M+H]^+$	0.7	137,161,163,178,233,261, 338
	24	His-Hyp	$C_{21}H_{24}N_4O_6$	429.1767	429.1769	$[M+H]^+$	-0.5	137,161,163,178,190,204,384
	25	Gln-Gln	$C_{20}H_{26}N_4O_7$	435.1870	435.1874	$[M+H]^+$	-0.9	
	26	Gln-Lys	$C_{21}H_{30}N_4O_6$	435.2235	435.2238	$[M+H]^+$	-0.7	
	27	Glu-Gln	$C_{20}H_{25}N_3O_8$	436.1719	436.1714	$[M+H]^+$	1.1	137,161,163,178,204,218, 232,287
	28	Tyr-Pro	$C_{24}H_{26}N_2O_6$	439.1865	439.1864	$[M+H]^+$	0.2	
	29	Val-Tyr	$C_{24}H_{28}N_2O_6$	441.2021	441.2020	$[M+H]^+$	0.2	137,161,163,178,190,218,232,262
	30	Ser-Trp	$C_{24}H_{25}N_3O_6$	452.1818	452.1816	$[M+H]^+$	0.4	137,161,163,178,250,323
	31	Gln-Phe	$C_{24}H_{27}N_3O_6$	454.1976	454.1972	$[M+H]^+$	0.9	
	32	Trp-Val	$C_{26}H_{29}N_3O_5$	464.2180	464.2179	$[M+H]^+$	0.2	
	33	Tyr-Gln	$C_{24}H_{27}N_3O_7$	470.1917	470.1917	$[M+H]^+$	0	137,161,163,178,218,232
	34	Tyr-Lys	$C_{25}H_{31}N_3O_6$	470.2280	470.2285	$[M+H]^+$	-1.1	
	35	Methylamine	$C_{11}H_{13}NO_2$	192.1020	192.1019	$[M+H]^+$	0.5	
Others	36	Ethylamine	$C_{12}H_{15}NO_2$	206.1176	206.1176	$[M+H]^+$	0.0	137,151,161,163,178
	37	Gly	$C_{12}H_{13}NO_4$	236.0917	236.0917	$[M+H]^+$	0.0	137,161,163,178,190,204

38	2-Methylbutylamine	$C_{15}H_{21}NO_2$	248.1646	248.1645	$[M+H]^+$	0.4	137,161,163,178,190,204,218
39	Ala	$C_{13}H_{15}NO_4$	250.1073	250.1074	$[M+H]^+$	-0.4	137,161,163,178,190,204,218,232
40	GABA	$C_{14}H_{17}NO_4$	264.1230	264.1230	$[M+H]^+$	0.0	137, 161,163,178,191,209
41	Ser	$C_{13}H_{15}NO_5$	266.1023	266.1023	$[M+H]^+$	0.0	
42	Histamine	$C_{15}H_{17}N_3O_2$	272.1394	272.1394	$[M+H]^+$	0.0	111,137,161,163,178,204
43	Glu	$C_{15}H_{17}NO_6$	308.1128	308.1129	$[M+H]^+$	-0.3	131,137,148,161,163,178,262
44	Ala-Ala-Ala	$C_9H_{17}N_3O_4$	392.1816	392.1816	$[M+H]^+$	0	
45	Leu-Gly-Gly	$C_{10}H_{19}N_3O_4$	406.1973	406.1974	$[M+H]^+$	-0.2	

Reference

1. S. Guo, W. Tang, Y. Hu, Y. Chen, A. Gordon, B. Li and P. Li, *Anal. Chem.*, 2020, **92**, 1431-1438.